ACS OMEGA

http://pubs.acs.org/journal/acsodf
Article

Lanthanide (Substituted-)Cyclopentadienyl Bis(phosphinimino)methanediide Complexes: Synthesis and Characterization

Fan Li, Yin-Cong Kong, Zi Yang, and Chen Wang*

Cite This: *ACS Omega* 2024, 9, 50830–50837

ABSTRACT: Design and synthesis of high-performance single-molecule magnets (SMMs) have long been a research focus. Inspired by the best dysprosium(III) metallocene SMMs and dysprosium(III) bis(methanediide) SMMs, we assumed dysprosium SMMs, which had electrical neutrality by combining the two types of ligands. As the Dy^{3+} center is coordinated by one (substituted-)cyclopentadienyl (Cp^R) ligand and one methanediide ($\{C(PPh_2NSiMe_3)_2\}^{2-}$) ligand on the axial sites, this ideal structure with linear $C_{carbene}$−Dy−Cp_{cent} would strengthen the magnetic anisotropy and exhibit excellent SMM properties. However, it is not easy to synthesize it in this configuration. We for the first time obtained $[Y\{C(PPh_2NSiMe_3)_2\}(Cp^R)(THF)]$ (Cp^R = Cp(**1**), Cp^{tBu}(**2**), Cp*(**3**), Cp = C_5H_5, Cp^{tBu} = C_5H_4tBu, Cp* = C_5Me_5) through the reactions of NaCp/KCp^R and $[Y\{C(PPh_2NSiMe_3)_2\}(I)(THF)_2]$. In the molecular structures of **1**−**3**, except for the two expected ligands, one coordination tetrahydrofuran (THF) molecule was also found in each complex. The P−C−P values of **1**−**3** were 135.46(7), 136.421(8), and 131.43(10)°, respectively, which were far less than 180°. The $C_{carbene}$−Y−Cp_{cent} of **1**−**3** deviated significantly from the linear shape, which was 118.021, 129.459, and 118.331°, respectively. Such a coordination environment makes the dysprosium congener $[Dy\{C(PPh_2NSiMe_3)_2\}(Cp^*)(THF)]$ (**4**) whose $C_{carbene}$−Dy−Cp_{cent} (118.295°) was too small to maintain axiality and which almost exhibited no SMM properties. Even though the first exploration of lanthanide (substituted-)cyclopentadienyl bis(phosphinimino)methanediide complexes did not live up to our expectation, it provided great experiences for the future success of high-performance lanthanide (substituted-)cyclopentadienyl methanediide SMMs.

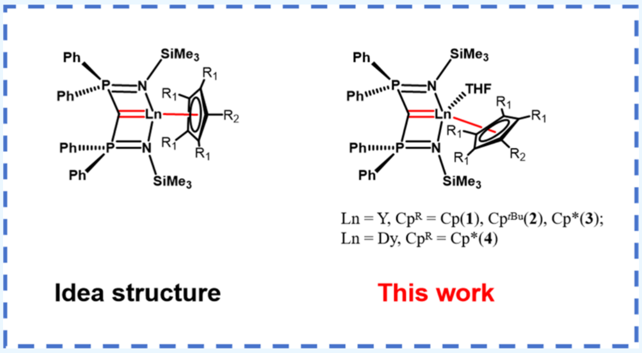

INTRODUCTION

Single-molecule magnets (SMMs) have attracted much attention for their potential application in high-density information storage, molecular spintronics, and quantum computing.[1−3] The first SMM (Mn_{12})[4] and many early-stage SMMs[5−8] are based on transition metals. However, in the recent two decades, there has been an exponential increase in the number of publications on lanthanide SMMs[9−16] for their easy-to-get magnetic anisotropy, which is essential for improving SMM properties.[17] SMM is also a coordination complex. How to regulate the magnetic anisotropy of lanthanide ions through different ligands has attracted organolanthanide chemistry researchers' interest.

Among the best-performing Ln-SMMs, a lot of them are dysprosium single-ion magnets (SIMs), which also were mononuclear lanthanide coordination compounds or organometallics, giving us a chance for understanding the magneto-structural correlations and designing high-performance SMMs.[17] Substituted or unsubstituted cyclopentadienyl, here abbreviated as Cp^R, has been applied in many lanthanide complexes for its rigid ring and concentrated charge. Layfield and Mills used the Cp^{ttt} (Cp^{ttt} = $C_5H_2tBu_3$) ligand and weakened the equatorial coordination to synthesize dysprosium(III) metallocene SMMs,[18,19] which was a breakthrough in that time. Then, they extended the dysprosium(III) metallocene series[20−24] by regulating the substituted group on Cp^R and made $[(Cp^{iPr5})Dy(Cp^*)]^+$[23] (Cp^{iPr5} = C_5iPr_5, Cp* = C_5Me_5) the best mononuclear SMMs by now. Gao, Tong, and Zheng used the steric bulk monodentate N-ligand or O-ligand to reinforce the axiality for oblate Dy^{III},[25−29] which were successful for building high-performance SMMs. Introducing Ln−N/C multiple bonds[30−32] in the axial axis would be advantageous for improving SMM behaviors. Liddle, who has made much contribution in the field of Ln−C multiple bonds (mainly pincer-type lanthanide carbene complexes),[32,33]

Received: October 27, 2024
Revised: November 20, 2024
Accepted: November 27, 2024
Published: December 13, 2024

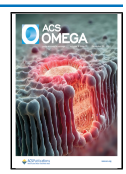

https://doi.org/10.1021/acsomega.4c09784
ACS Omega 2024, 9, 50830−50837

Scheme 1. Synthesis of Complexes 1−3 from the Compound [Y{C(PPh$_2$NSiMe$_3$)$_2$}(I)(THF)$_2$]

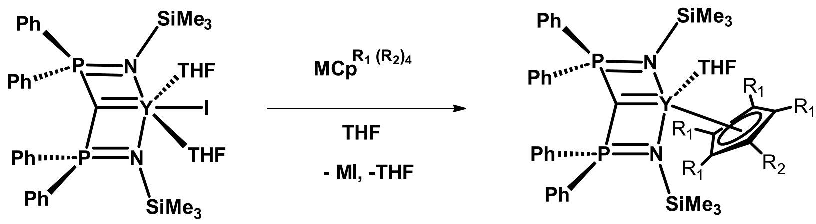

brought in the methanediide dianion and constructed SMMs characterized with almost linear C = Dy = C units with short average Dy−C distances, supporting the hypothesis that a more linear axial ligand field with shorter M−L distances produces enhanced SMM properties.[34,35] However, all of the reported Ln-SMMs are not good enough for practical use. There has been an impetus toward the search for a new coordination environment of Ln-SMMs.

The above strategies inspired us to construct possible high-performance Ln-SMMs, which employed one Cp^R ligand and one methanediide ligand on the axial sites to strengthen the magnetic anisotropy. This will be a remarkable challenge for synthetic chemists to keep this geometry. Here, we report our progress on this hypothesis. The raw materials were replaced by semblable yttrium complexes to explore the synthesis route because Y^{3+} and Dy^{3+} show similar chemical properties and yttrium complexes are diamagnetic for monitoring the reaction. Through the reactions of alkali metal cyclopentadienide and yttrium iodide [Y{C(PPh$_2$NSiMe$_3$)$_2$}(I)(THF)$_2$],[36] we successfully obtained [Y{C(PPh$_2$NSiMe$_3$)$_2$}(Cp^R)(THF)] (Cp^R = Cp(**1**), Cp^{tBu}(**2**), Cp*(**3**), Cp = C_5H_5, Cp^{tBu} = C_5H_4tBu). Due to the coordination of tetrahydrofuran (THF), the C$_{carbene}$−Y−Cp$_{cent}$ of **1−3** deviated significantly from the linear shape, which was 118.021, 129.459, and 118.295°, respectively. Only the dysprosium congener of **3**, [Dy{C(PPh$_2$NSiMe$_3$)$_2$}-(Cp*)(THF)] (**4**), was isolated. The C$_{carbene}$−Dy−Cp$_{cent}$ (118.295°) is too small to maintain axiality, which made **4** exhibit almost no SMM properties.

■ RESULTS AND DISCUSSION

Synthesis and Spectroscopic Characterization. We first investigated Cp, since it has less steric bulk and is easily obtained, to determine the feasibility of our methodology. The yttrium bis(phosphinimino)methanediide complex [Y{C-(PPh$_2$NSiMe$_3$)$_2$}(I)(THF)$_2$] was treated with NaCp. ^{1}H NMR and ^{31}P{^{1}H}NMR spectral monitoring of the reaction in C_6D_6 and a few drops of d_8-THF showed the formation of new complexes **1** at room temperature. The scaled-up reaction in THF provided mononuclear yttrium complexes [Y{C-(PPh$_2$NSiMe$_3$)$_2$}(Cp)(THF)] (**1**) in 43% yields (Scheme 1). With our methodology established, we then investigated synthesizing the yttrium analogue with bulk-substituted cyclopentadienyl. Cp^{tBu} and Cp* were selected and successfully adapted in this way. [Y{C(PPh$_2$NSiMe$_3$)$_2$}(Cp^{tBu})(THF)] (**2**) was obtained in 46% yields with heating at 50 °C, while [Y{C(PPh$_2$NSiMe$_3$)$_2$}(Cp*)(THF)] (**3**) was obtained in 28% yields at 75 °C (Scheme 1). The complexes **1−3** were characterized by NMR spectroscopy (Figures S1−S9) and elemental analysis (EA). The ^{1}H NMR spectra of **1−3** each exhibit signals for Cp^R fragments (δ_H: **1**, 6.75 (s, 5H, Cp); **2**, 6.73 (t, $^3J_{HH}$ = 2.5 Hz, 2H, Cp^{tBu}−C*H*), 6.22 (t, $^3J_{HH}$ = 2.7 Hz, 2H, Cp^{tBu}−C*H*), 1.59 (s, 9H, Cp^{tBu}-C*Me*$_3$); **3**, 2.23(Cp*-*Me*)). Their ^{13}C{^{1}H} NMR spectra contain a distinctive doublet of triplet signals for the methanediides due to ^{31}P and ^{89}Y coupling (δ_C: **1**, 51.4, $^1J_{CP}$ = 131.2 Hz, $^1J_{CY}$ = 6.2 Hz; **2**, 54.6, $^1J_{CP}$ = 137.5 Hz, $^1J_{CY}$ = 7.5 Hz; **3**, 53.7, $^1J_{CP}$ = 123.8 Hz, $^1J_{CY}$ = 8.8 Hz) (Table 1), and ^{89}Y coupling is observed in their ^{31}P{^{1}H} NMR spectra (δ_P: **1**, 3.2, d, $^2J_{PY}$ = 12.0 Hz; **2**, 5.8, d, $^2J_{PY}$ = 14.0 Hz; **2**, 5.9, d, $^2J_{PY}$ = 14.0 Hz) (Table 1). These resonances are comparable to the corresponding data for [Y{C(PPh$_2$NSiMe$_3$)$_2$}(I)(THF)$_2$] (δ_C 60.28, $^1J_{CP}$ = 207 Hz, $^1J_{CY}$ = 5 Hz; δ_P 3.48, $^2J_{PY}$ = 13 Hz)[36] and other complexes of the general formula [Y{C(PPh$_2$NSiMe$_3$)$_2$}(X)(THF)] (X = anionic ligand).[37−40] The four complexes were characterized by elemental analysis (EA), where EA values obtained are >0.5% out from expected values, maybe due to the uncertainty of residual toluene.

Table 1. Characteristic NMR Data of Complexes 1−3 in C_6D_6 at 25 °C

comp.	^{13}C{^{1}H}: Ln = *C* (ppm)	^{31}P{^{1}H}: Ln = C−*P* (ppm)
1	51.4 (td, $^1J_{CP}$ = 131.2 Hz, $^1J_{CY}$ = 6.2 Hz)	3.2 (d, $^2J_{PY}$ = 12.0 Hz)
2	54.6 (td, $^1J_{CP}$ = 137.5 Hz, $^1J_{CY}$ = 7.5 Hz)	5.8 (d, $^2J_{PY}$ = 14.0 Hz)
3	53.7 (td, $^1J_{CP}$ = 123.8 Hz, $^1J_{CY}$ = 8.8 Hz)	5.9 (d, $^2J_{PY}$ = 14.0 Hz)

We tried to expend these synthetic methods to the dysprosium congeners of the three yttrium (substituted-)cyclopentadienyl methanediide complexes, but only one complex [Dy{C(PPh$_2$NSiMe$_3$)$_2$}(Cp*)(THF)] (**4**) was isolated in total yields of 27% (Scheme 2). One of the main reasons probably was that the proposed intermediates "[Dy(Bn)$_2$(I)(THF)$_3$]" (Bn = $CH_2C_6H_5$) and "[Dy{C-(PPh$_2$NSiMe$_3$)$_2$}(I)(THF)$_2$]", which were unsuccessfully isolated,[41] are too active. It may need more harsh synthetic conditions to obtain dysprosium congeners of **1−2**. As for the synthesis of **4** (or **3**), which needs a higher temperature (75 °C) than **1** and **2**, the properties of Cp* may be another reason for the success of the isolation of **4**. Complex **4** was characterized by elemental analysis.

Structural Characterization. Crystals of **1−4** were formed from a toluene solution and proved suitable for structural determination by single-crystal X-ray diffraction. Both complexes **1** and **2** were crystallized in the monoclinic

https://doi.org/10.1021/acsomega.4c09784
ACS Omega 2024, 9, 50830−50837

Scheme 2. Synthesis of Complex 4

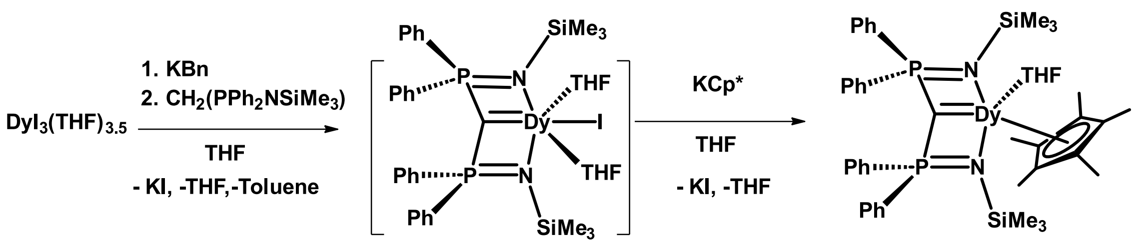

space group $P2_1/c$, while **3** and **4** were crystallized in the monoclinic space group $P2_1/n$ (Table S1). Molecular structures of **1**−**4** are shown in Figures 1−4. The coordination environment of each center ion (Y^{3+} in **1**−**3** or Dy^{3+} in **4**) is composed of one η^5-cyclopentadienyl ligand (Cp, Cp^{tBu}, or Cp*), one tridentate bis(phosphinimino)methanediide ($\{C(PPh_2NSiMe_3)_2\}^{2-}$), and one coordinated monodentate THF molecule. The $\{C(PPh_2NSiMe_3)_2\}^{2-}$ dianion coordinates to the lanthanide center through C and P atoms. In complexes **1**−**3**, the Y−$C_{carbene}$ (or Y−C16) bond lengths are 2.4260(12), 2.4446(13), and 2.4381(16) Å, respectively (Table 2). The $\{C(PPh_2NSiMe_3)_2\}^{2-}$ intraligand bond lengths and angles are consistent with previously reported Y(III) methanediide.[36−40] It is noteworthy that the P−C−P angle (**1**, 135.46(7)°; **2**, 136.42(8); **3**, 131.43(10)°) exhibited a significant deviation from the planarity of the pincer ligand scaffold compared with $[Y\{C(PPh_2NSiMe_3)_2\}(I)(THF)_2]$ (172.5(2)°)[36] and $[Y\{C(PPh_2NSiMe_3)_2\}_2]^-$ (168.9(2), 169.4(2)),[34] giving the diagnostic pseudoboat conformation. However, this phenomenon was also found in complexes $[Y\{C(PPh_2NSiMe_3)_2\}(X)(THF)]$ (135.5(3)−139.24(14)°).[37−40] The Y−$C_{carbene}$ bond length of **1**−**3** is slightly longer in comparison with the distances reported for $[Y\{C(PPh_2NSiMe_3)_2\}(I)(THF)_2]$ (2.356(3) Å).[36] The distances of Y^{3+} to the cyclopentadienyl center (Y−Cp_{cent}) in **1**−**3** are 2.391, 2.423, and 2.421 Å, respectively (Table 2), which is not quite affected with the substituted group on the ring. Compared with the reported yttrium (substituted-)cyclopentadienyl complexes, the Y−Cp_{cent} distance in **1** is obviously shorter by ca. 0.3 Å.[42] The Y−Cp_{cent} distance in **3** was in accordance with $[Cp^*Y(NC_6H_3(CF_3)_2\text{-}3,5)(THF)_2]_2$.[43] No structure data about Y−Cp^{tBu} was found in the literature. The bite angles $C_{carbene}$−Y−Cp_{cent} of 118.021, 129.459, and 118.331° are found for **1**−**3**, respectively (Table 2). It is noteworthy that the increased steric bulk from Cp to Cp* only makes the $C_{carbene}$−Y−Cp_{cent} enlarged by 0.31°. While comparing Cp^{tBu} with Cp, the angle of $C_{carbene}$−Y−Cp_{cent} is obviously increased by ca. 11.4°. This observation can be attributed to the one *t*Bu group which makes the Cp^{tBu} ring lean to the pincer methanediide ($C_{carbene}$−Y−C_{CtBu} = 104.65(4)°). Thus, the $C_{carbene}$−Y−Cp_{cent} angle is enlarged in turn.

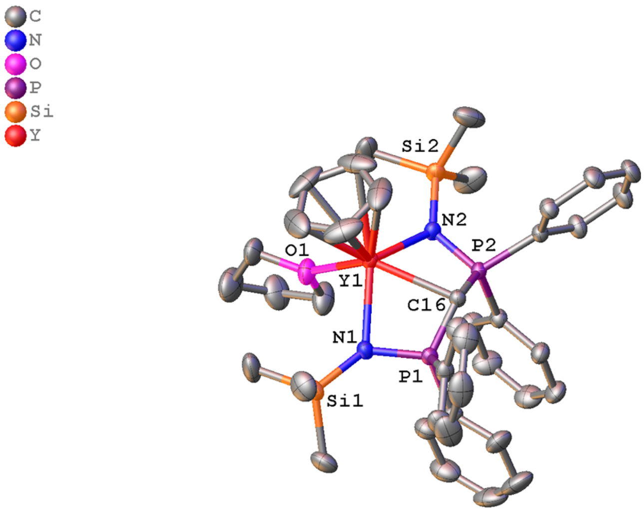

Figure 1. Molecular structure of **1** with thermal ellipsoids at a 30% probability. All hydrogen atoms are omitted for clarity. Selected bond lengths (Å) and angles (deg): Y1−N1 2.3443(10); Y1−N2 2.3573(10); Y1−C16 2.4260(12); Y1−$\mathbf{C}_{Cp}$: 2.6450(16), 2.6811(16), 2.6635(17), 2.6889(16), 2.6337(17), respectively; Y1−O1 2.375(4); Y1−O1A 2.414(11); P1−N1 1.6340(11); P1−C16 1.6694(11); P2−N2 1.6304(10); P2−C16 1.6681(12); O1−Y1−C16 132.50(12); O1A−Y1−C16 131.3(3); N1−Y1−N2 121.54(4); N1−Y1−C16 68.25(4); N1−Y1−O1 93.0(4); N1−Y1−O1A 93.9(9); N2−Y1−C16 67.88(4); N2−Y1−O1 89.4(3); N2−Y1−O1A 87.4(9); P1−C16−P2 135.46(7); P1−C16−Y1 89.84(5); P2−C16−Y1 89.83(5).

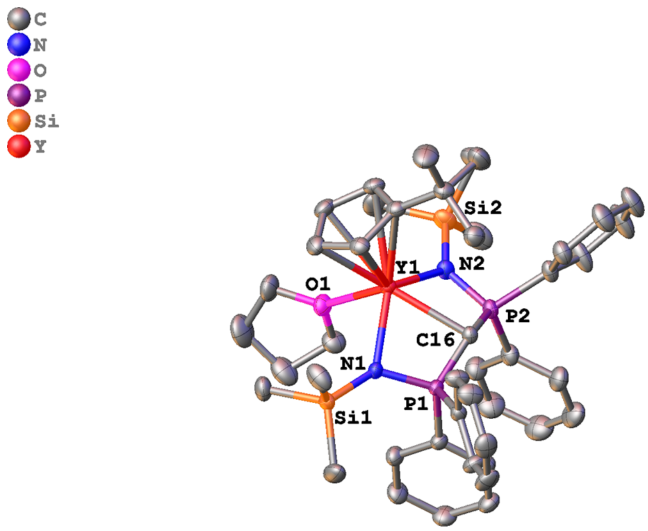

Figure 2. Molecular structure of **2** with thermal ellipsoids at a 30% probability. All hydrogen atoms are omitted for clarity. Selected bond lengths (Å) and angles (deg): Y1−O1 2.3856(11); Y1−N1 2.3368(11); Y1−N2 2.3618(12); Y1−C16 2.4446(13); Y1−$\mathbf{C}_{Cp}$: 2.7023(14), 2.6626(14), 2.7809(14), 2.7290(14), 2.6490(14), respectively; Y1−O1 2.3856(11); P1−N1 1.6324(11); P1−C16 1.6734(13); P2−N2 1.6295(12); P2−C16 1.6765(13); O1−Y1−C16 124.20(4); N1−Y1−N2 122.50(4); N1−Y1−C16 68.15(4); N1−Y1−O1 88.03(4); N2−Y1−C16 67.46(4); N2−Y1−O1 88.09(4); P1−C16−P2 136.42(8); P1−C16−Y1 89.02(5); P2−C16−Y1 90.33(5).

Complexes **3** and **4** share the same coordinate ligands. In **4**, if we treat Cp* as a point charge in the ring center, the geometry of the Cp* center and other three coordinate atoms

https://doi.org/10.1021/acsomega.4c09784
ACS Omega 2024, 9, 50830−50837

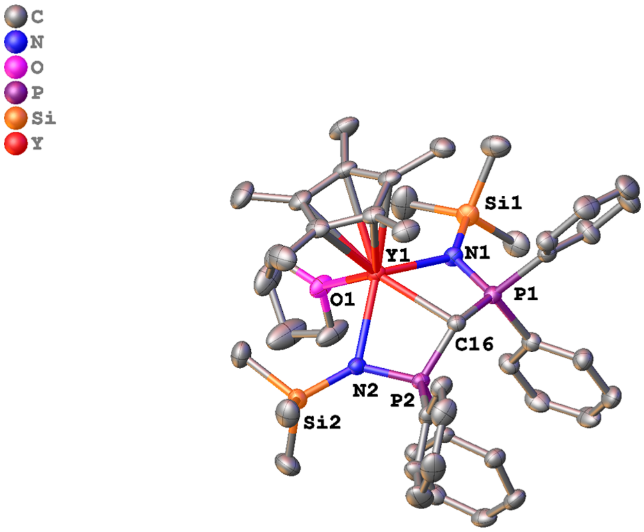

Figure 3. Molecular structure of **3** with thermal ellipsoids at a 30% probability. All hydrogen atoms are omitted for clarity. Selected bond lengths (Å) and angles (deg): Y1−N1 2.4024(14); Y1−N2 2.3912(13); Y1−C16 2.4381(16); Y1−C_{Cp}: 2.6782(17), 2.6983(17), 2.6776(16), 2.7458(17), 2.7245(17), respectively; Y1−O1 2.4034(12); P1−N1 1.6382(14); P1−C16 1.6751(16); P2−N2 1.6304(10); P2−C16 1.6739(16); O1−Y1−C16 129.54(5); N1−Y1−N2 116.71(5); N1−Y1−C16 67.81(5); N1−Y1−O1 89.50(5); N2−Y1−C16 67.30(5); N2−Y1−O1 86.59(5); P1−C16−P2 131.43(10); P1−C16−Y1 90.37(7); P2−C16−Y1 90.67(7).

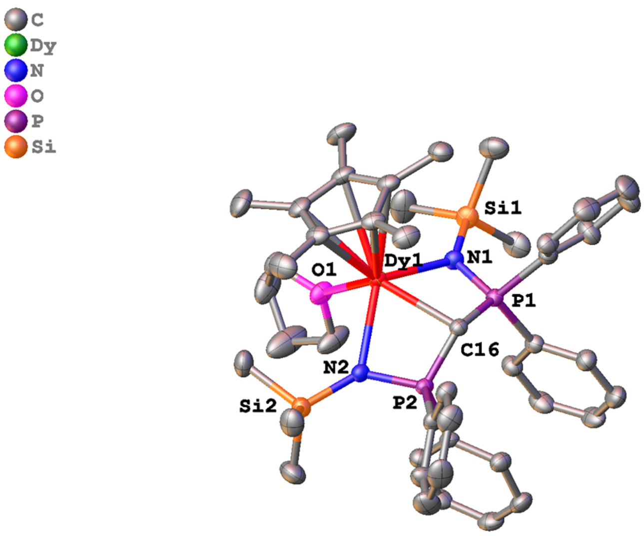

Figure 4. Molecular structure of **4** with thermal ellipsoids at a 30% probability. All hydrogen atoms are omitted for clarity. Selected bond lengths (Å) and angles (deg): Dy1−N1 2.4025(15); Dy1−N2 2.3928(14); Dy1−C16 2.4336(17); Dy1−C_{Cp}: 2.6836(17), 2.7510(17), 2.7082(18), 2.7308(18), 2.6865(18), respectively; Dy1−Cpcent 2.429; Dy1−O1 2.4257(13); P1−N1 1.6334(15); P1−C16 1.6756(17); P2−N2 1.6319(15); P2−C16 1.6750(17); Cp_{cent}−Dy1−C16 118.295; O1−Dy1−C16 129.47(5); N1−Dy1−N2 116.64(5); N1−Dy1−C16 67.81(5); N1−Dy1−O1 67.60(5); N2−Dy1−C16 67.19(5); N2−Dy1−O1 86.63(5); P1−C16−P2 131.59(10); P1−C16−Dy1 90.68(7); P2−C16−Dy1 90.98(7).

would be a distorted pyramid. The Dy−$C_{carbene}$ bond length is 2.4336(17) Å, which is slightly longer than that of [Dy{C(PPh$_2$NSiMe$_3$)$_2$}{CH(PPh$_2$NSiMe$_3$)$_2$}] (2.3670 Å) but comparable with that of [Dy{C(PPh$_2$NSiMe$_3$)$_2$}$_2$][K(18C6)(THF)$_2$] (2.434(6) and 2.433(6) Å).[34] The Dy−Cp_{cent} distance is 2.429 Å (Table 2), which is slightly longer than that of [Dy(DAD)Cp*(THF)] (DAD: [2,6-*i*Pr$_2$C$_6$H$_3$N−CMe = CM−NC$_6$H$_3$*i*Pr$_2$-2,6] (2.391(2) Å)).[44] The angle $C_{carbene}$−Dy−Cp_{cent} is 118.295°, showing poor axiality. The shortest distance between the neighboring Dy^{3+} ions is 11.304 Å.

Table 2. Selected Bond Lengths (Å) and Angles (deg) of Complexes 1−3

comp.	Ln−$C_{carbene}$	Ln−Cp_{cent}	$C_{carbene}$−Ln−Cp_{cent}
1(Y)	2.4260(12)	2.391	118.021
2(Y)	2.4446(13)	2.423	129.459
3(Y)	2.4381(16)	2.421	118.331
4(Dy)	2.4336(17)	2.429	118.295

Magnetic Characterization. To explore the magnetic behavior of **4**, static susceptibility measurements were performed under a direct current (1 kOe, dc) magnetic field over the temperature range from 2 to 300 K (Figure 5). The product ($\chi_m T$) value of temperature-dependent magnetic susceptibility and temperature at 300 K was 13.29 cm^3 mol^{-1} K, close to those expected for one free Dy^{3+} ion with ground terms of $^6H_{15/2}$ ($g = 4/3$, $\chi_m T = 14.17$ cm^3 mol^{-1} K). the $\chi_m T$ values declined slowly with a decrease in temperature initially, then exhibited a sudden drop below 3 K to a minimum of 5.88 cm^3 mol^{-1} K at 2 K. The zero-field-cooled/field-cooled (ZFC/FC) magnetizations (Figure S10) showed no clear divergences below 10 K. No magnetic hysteresis loop was found in the range of −50 to 50 kOe at 2 K with a field sweep speed of 500 Oe/s (Figures 6 and S11), proving poor/no SMM magnetic properties. The $M(H)$ at 2 K saturates at a value of 4.55 β mol^{-1} (Figure S12). This value is a little lower than the expected saturation value of 5.23 β, which is likely due to crystal-field effects and low-lying excited states. The unsaturated magnetization together with the superimposed M vs HT^{-1} curves (Figure 6) at varying temperatures indicates the poor magnetic anisotropy in the systems.[45]

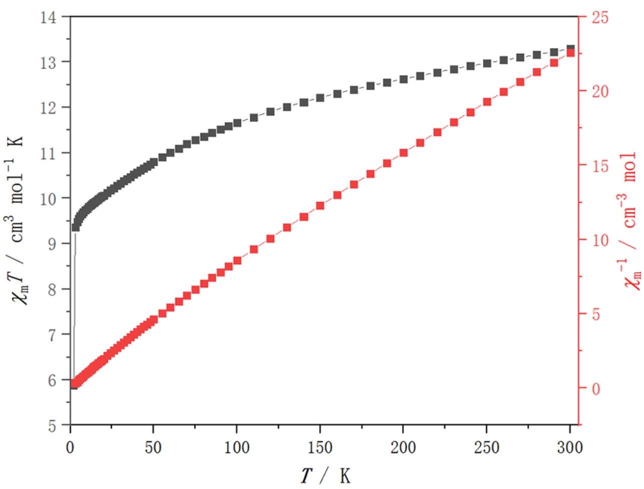

Figure 5. Temperature dependence of $\chi_m T$ or χ_m^{-1} for **4** under a 1 kOe dc magnetic field.

We performed dynamic susceptibility measurements at nearly zero dc field to investigate further the magnetic behaviors of complex **4**. No peak was observed in the out-of-phase alternating current susceptibilities (χ_m'') vs T plots at different frequencies (Figure S13), meaning that complex **4** did

https://doi.org/10.1021/acsomega.4c09784
ACS Omega 2024, 9, 50830−50837

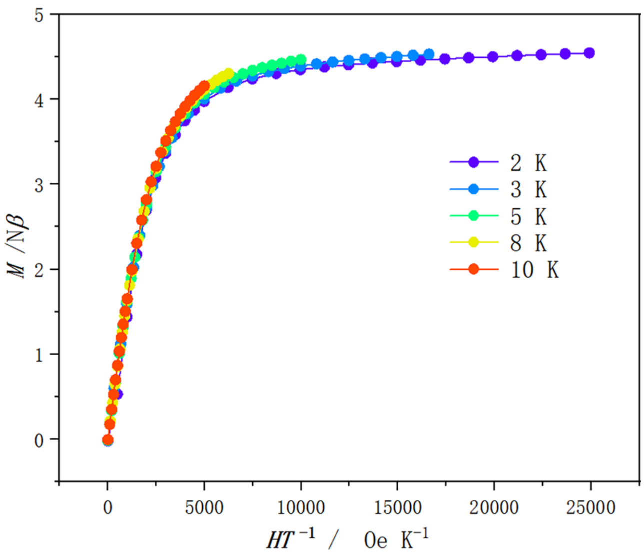

Figure 6. M vs HT^{-1} plots at different temperatures for **4**.

not behave like SMMs (as the data at 100 Hz fluctuated along a line, the peaks at this frequency were meaningless; the data above 100 Hz were counted). An obvious increase of χ_m'' as temperature declined below 7 K was attributable to unsuppressed quantum tunneling magnetization (QTM). These results were also in accordance with those of the dc measurements.

Compared with the Dy SMMs sharing the Dy = C bond, like [Dy{C(PPh$_2$NSiMe$_3$)$_2$}{CH(PPh$_2$NSiMe$_3$)$_2$}] (effective energy barrier: U_{eff} = 177 cm^{-1}) and [Ln{C(PPh$_2$NSiMe$_3$)$_2$}$_2$]-[K(18C6)(THF)$_2$] (U_{eff} = 501 and 565 cm^{-1}),[34] no U_{eff} was observed in **4**. Dy SMM with one Cp* ligand such as [Dy(DAD)Cp*(THF)] (U_{eff} = 254 cm^{-1})[44] is also better than **4**. *Ab initio* calculation about complex **4** exhibited that the M_J states are highly mixed (Table S2). The magnetic relaxation through the first excited state could not be discovered for the high possibility (0.330) of quantum tunneling magnetization (Figure S14), which could explain why no U_{eff} was observed in the absence of a dc field.

■ CONCLUSIONS

In summary, we successfully developed salt elimination/metathesis protocols to obtain three different heteroleptic yttrium complexes [Y{C(PPh$_2$NSiMe$_3$)$_2$}(Cp^R)(THF)] (Cp^R=Cp(**1**), Cp^{tBu}(**2**), Cp*(**3**)) by using [Y{C-(PPh$_2$NSiMe$_3$)$_2$}(I)(THF)$_2$] as precursors. This synthetic route was also extended to obtain [Dy{C(PPh$_2$NSiMe$_3$)$_2$}-(Cp*)(THF)] (**4**), as the combination of {C-(PPh$_2$NSiMe$_3$)$_2$}$^{2-}$ and Cp^R in **1**−**4** did not provide sufficient steric bulk to exclude THF from the coordination sphere of the lanthanide ions. The C$_{carbene}$−Y−Cp$_{cent}$ of **1**−**4** is 118.021, 129.459, 118.331, and 118.295°, respectively, showing low axiality. As a result, the magnetic behaviors of **4** are far from SMMs. We have attempted to remove the solvent by heating a solid sample in vacuo for hours. But analysis of the NMR spectra of the resultant solid revealed that THF could not be removed without destroying the coordination unit "Y{C-(PPh$_2$NSiMe$_3$)$_2$}(Cp^R)". Carefully regulating the appropriate steric effect and charge effect of the two ligands {C-(PPh$_2$NSiMe$_3$)$_2$}$^{2-}$ and Cp^R would be useful to enlarge the C$_{carbene}$−Y−Cp$_{cent}$ angle, making them near the idea Y{C-(PPh$_2$NSiMe$_3$)$_2$}(Cp^R) unit with a C$_{carbene}$−Y−Cp$_{cent}$ angle of 180°. Next, we would conduct further studies in this direction to produce high-performance SMMs.

■ EXPERIMENTAL SECTION

General. All operations were carried out under an atmosphere of argon by using Schlenk techniques or in an argon-filled glovebox. Toluene, THF, hexane, and C$_6$D$_6$ were dried over the Na/K alloy, transferred under vacuum, and stored in the glovebox. The raw materials [Y{C-(PPh$_2$NSiMe$_3$)$_2$}(I)(THF)$_2$],[36] DyI$_3$(THF)$_{3.5}$,[46] KBn,[47] NaCp,[48] KCp*,[49] CH$_2$(PPh$_2$NSiMe$_3$)$_2$,[50] and C$_5$H$_5$tBu[51] were synthesized following the literature. KCp^{tBu} was synthesized by slowly adding a solution of KN(SiMe$_3$)$_2$ (1.63 g, 8.18 mmol) in THF (ca. 10 mL) to a solution of C$_5$H$_5$*t*Bu (1.00 g, 8.18 mmol) in THF (ca. 10 mL). After 5 h, KCp^{tBu} was isolated by removing the volatiles under vacuum and repeatedly washed with hexane. Brown KCp^{tBu} (0.81 g, 62%) was dried in vacuum. ^{1}H NMR (500 MHz, C$_6$D$_6$, 25 °C): δ = 5.70 (m, 2H, Cp^{tBu}−C*H*), 5.67 (m, 2H, Cp^{tBu}−C*H*), 1.37 (s, 9H, Cp^{tBu}−C*Me*$_3$). These compounds were stored in the glovebox. ^{1}H, ^{13}C{^{1}H}, and ^{31}P{^{1}H} NMR spectra were recorded on a Bruker Avance III HD 500 MHz spectrometer. Chemical shifts were reported in δ units with references to the residual solvent resonance of the deuterated solvents for proton and carbon chemical shifts and to external H$_3$PO$_4$ (85%) for phosphorus chemical shifts. Fourier-transform infrared spectroscopy (FTIR) spectra were recorded on a Bruker α II spectrometer placed in a glovebox. EA values were obtained from an Elementar UNICUBE analyzer.

*Synthesis of [Y{C(PPh$_2$NSiMe$_3$)$_2$}(Cp)(THF)] (**1**).* [Y{C-(PPh$_2$NSiMe$_3$)$_2$}(I)(THF)$_2$] (274 mg, 0.30 mmol) and NaCp·0.25THF (32 mg, 0.30 mmol) were mixed in a vial with 5 mL of THF. After stirring at room temperature overnight, the precipitate was separated by centrifugation. The volatiles were removed under vacuum. The solid was recrystallized from toluene to afford **1** (0.5Toluene) as yellow crystals. Yield: 106 mg, 43%. ^{1}H NMR (500 MHz, C$_6$D$_6$, 25 °C): δ = 8.30 (dd, $^3J_{PH}$ = 13.0 Hz, $^3J_{HH}$ = 7.0 Hz, 4H, *o*-P*Ph*$_2$), 7.26 (t, $^3J_{HH}$ = 7.2 Hz 4H, *m*-P*Ph*$_2$), 7.19 (m, 2H, *p*-P*Ph*$_2$), 7.16−7.13 (m, toluene-*Ph* overlapped with the residual solvent resonance of the deuterated solvent), 7.10 (m, 4H, *o*-P*Ph*$_2$), 7.02 (m, 1H, toluene-*Ph*), 6.84 (t, $^3J_{HH}$ = 7.2 Hz, 2H, *p*-P*Ph*$_2$), 6.75 (s, 5H, *Cp*), 6.71 (t, $^3J_{HH}$ = 7.5 Hz, 4H, *m*-P*Ph*$_2$), 3.86 (m, 4H, THF-OC*H*$_2$), 2.11 (s, 1.5H, toluene-*Me*),1.37 (m, 4H, THF−C*H*$_2$), 0.00 (s, 18H, Si*Me*$_3$). ^{13}C{^{1}H} NMR (125 MHz, C$_6$D$_6$, 25 °C): δ = 142.5 (t, $^1J_{CP}$ = 56.8 Hz, *i*-P*Ph*$_2$), 137.5 (toluene-*Ph*), 135.7 (t, $^1J_{CP}$ = 41.9 Hz, *i*-P*Ph*$_2$), 131.4 (t, $^2J_{CP}$ = 5.6 Hz, *o*-P*Ph*$_2$), 130.8 (t, $^2J_{CP}$ = 5.0 Hz, *o*-P*Ph*$_2$), 129.1 (*p*-P*Ph*$_2$), 129.0 (toluene-*Ph*), 128.21 (toluene-*Ph*), 128.19 (*p*-P*Ph*$_2$), 126.8 (t, $^3J_{CP}$ = 5.6 Hz, *m*-P*Ph*$_2$), 125.3 (toluene-*Ph*), 111.03 (s, *Cp*), 71.4 (THF-OCH$_2$), 51.4 (td, YCP, $^1J_{CP}$ = 131.2 Hz, J_{YC} = 6.2 Hz), 25.1 (THF-CH$_2$), 21.1 (toluene-*Me*), 3.8 (s, NSi*Me*$_3$). ^{31}P{^{1}H} NMR(202 MHz, C$_6$D$_6$, 25 °C): δ = 3.2 (d, $^2J_{P-Y}$ = 12.1 Hz). IR ν/cm^{-1}: 2185(w), 1559(w), 1481(w), 1435(m), 1358(w), 1270(s), 1240(s), 1157(w), 1109(m), 955(w), 916(w), 825(s), 800(m), 772(m), 737(s), 686(s), 631(m), 603(m), 573(m). Elemental analysis calcd (%) for C$_{40}$H$_{51}$N$_2$OP$_2$Si$_2$Y· 0.5Toluene: C, 63.03; H, 6.69; N, 3.38; found C, 63.51; H, 6.09; N, 3.48.

*Synthesis of [Y{C(PPh$_2$NSiMe$_3$)$_2$}(Cp^{tBu})(THF)] (**2**).* [Y{C-(PPh$_2$NSiMe$_3$)$_2$}(I)(THF)$_2$] (274 mg, 0.30 mmol) and KCp^{tBu} (48 mg, 0.30 mmol) were mixed in a vial with 5 mL

https://doi.org/10.1021/acsomega.4c09784
ACS Omega 2024, 9, 50830−50837

of THF. After stirring at room temperature for 2 h and another 2 h at 50 °C, the precipitate was separated by centrifugation. The volatiles were removed under vacuum. The solid was recrystallized from toluene to afford **2** as colorless crystals. Yield: 114 mg, 46%. ^{1}H NMR(500 MHz, C_6D_6, 25 °C): δ = 8.20 (m, 4H, *o*-P*Ph*$_2$), 7.27 (m, 4H, *m*-P*Ph*$_2$), 7.20 (m, 2H, *p*-P*Ph*$_2$), 6.97 (m, 4H, *o*-P*Ph*$_2$), 6.81(m, 2H, *p*-P*Ph*$_2$), 6.73 (t, $^{3}J_{HH}$ = 2.5 Hz, 2H, Cp^{tBu}−C*H*), 6.64 (m, 4H, *m*-P*Ph*$_2$), 6.22 (t, $^{3}J_{HH}$ = 2.7 Hz, 2H, Cp^{tBu}−C*H*), 3.92 (m, 4H, THF-OC*H*$_2$), 1.59 (s, 9H, Cp^{tBu}-C*Me*$_3$), 1.44 (m, 4H, THF−C*H*$_2$), 0.17 (s, 18H, NSi*Me*$_3$). ^{13}C{^{1}H} NMR(125 MHz, C_6D_6, 25 °C): δ = 142.3 (t, $^{1}J_{CP}$ = 55.6 Hz, *i*-P*Ph*$_2$), 141.5(Cp^{tBu}-CCMe$_3$), 137.6 (t, $^{1}J_{CP}$ = 41.2 Hz, *i*-P*Ph*$_2$), 132.4(P*Ph*$_2$), 130.6(P*Ph*$_2$), 129.1(P*Ph*$_2$), 128.2(P*Ph*$_2$), 127.0(P*Ph*$_2$), 126.6(P*Ph*$_2$), 109.6-(Cp^{tBu}-CH), 108.9(Cp^{tBu}-CH), 72.07 (br, THF-OCH$_2$), 54.6 (td, YCP, $^{1}J_{CP}$ = 137.5 Hz, $^{1}J_{CY}$ = 7.5 Hz), 33.0(Cp^{tBu}-C*Me*$_3$), 32.4(Cp^{tBu}-CMe$_3$), 25.0(THF-CH$_2$), 4.50(NSi*Me*$_3$). ^{31}P{^{1}H} NMR(202 MHz, C_6D_6, 25 °C): δ = 5.8 (d, $^{2}J_{PY}$ = 14.1 Hz). IR ν/cm^{-1}: 2185(w), 1581(w), 1481(w), 1436(m), 1403(w), 1262(s), 1235(s), 1177(w), 1124(w), 1104(m), 1061(w), 1028(w), 996(w), 860(m), 827(s), 797(s), 775(m), 734(s), 709(m), 691(s), 651(m), 631(m), 614(m), 573(m), 531(s). Elemental analysis calcd (%) for $C_{44}H_{59}N_2OP_2Si_2Y$: C, 62.99; H, 7.09; N, 3.34; found C, 62.37; H, 7.39; N, 3.25.

Synthesis of [Y{C(PPh$_2$NSiMe$_3$)$_2$}(Cp)(THF)] (**3**).* [Y{C-(PPh$_2$NSiMe$_3$)$_2$}(I)(THF)$_2$] (274 mg, 0.30 mmol) and KCp* (53 mg, 0.30 mmol) were mixed in a vial with 5 mL of THF. After stirring at room temperature for 2 h and another 8 h at 75 °C, the precipitate was separated by centrifugation. The volatiles were removed under vacuum. The solid was recrystallized from toluene to afford **3** (0.5Toluene) as colorless crystals. Yield: 76 mg, 28%. ^{1}H NMR (500 MHz, C_6D_6, 25 °C): δ = 8.38 (dd, $^{3}J_{HP}$ = 13.5 Hz, $^{3}J_{HH}$ = 7.0 Hz, 4H, *o*-P*Ph*$_2$), 7.33 (t, $^{3}J_{HH}$ = 7.5 Hz, 4H, *m*-P*Ph*$_2$), 7.22 (t, 2H, $^{3}J_{HH}$ = 7.5 Hz, *p*-P*Ph*$_2$), 7.13 (m, 1H, toluene-*Ph*), 7.02 (m, 1.5H, toluene-*Ph*), 6.94 (dd, $^{3}J_{HP}$ = 12.2 Hz, $^{3}J_{HH}$ = 7 Hz, 4H, *o*-P*Ph*$_2$), 6.79 (t, $^{3}J_{HH}$ = 7.5 Hz, 2H, *p*-P*Ph*$_2$), 6.61 (t, $^{3}J_{HH}$ = 7.5 Hz, 4H, *m*-P*Ph*$_2$), 4.14 (m, 4H, THF-OC*H*$_2$), 2.23 (s, 15H, Cp*-*Me*), 2.11 (s, 1.5H, toluene-*Me*), 1.48 (m, 4H, THF−C*H*$_2$), 0.12 (s, 18H, Si*Me*$_3$). ^{13}C{^{1}H} NMR (125 MHz, C_6D_6, 25 °C): δ = 142.8 (t, $^{1}J_{CP}$ = 58.1 Hz, *i*-P*Ph*$_2$), 137.5 (toluene-*Ph*), 137.2 (t, $^{1}J_{CP}$ = 39.4 Hz, *i*-P*Ph*$_2$), 132.81 (t, $^{2}J_{CP}$ = 5.6 Hz, *o*-P*Ph*$_2$), 131.0 (t, $^{2}J_{CP}$ = 5.6 Hz, *o*-P*Ph*$_2$), 129.1 (*p*-P*Ph*$_2$), 129.0 (toluene-*Ph*), 128.20 (toluene-*Ph*), 128.18 (*p*-P*Ph*$_2$), 126.9 (t, $^{3}J_{CP}$ = 5.6 Hz, *m*-P*Ph*$_2$), 126.6 (t, $^{3}J_{CP}$ = 5.6 Hz, *m*-P*Ph*$_2$), 125.31 (toluene-*Ph*), 117.82 (Cp*-CMe), 71.13 (br, THF-OCH$_2$), 53.7 (td, YCP, $^{1}J_{CP}$ = 123.8 Hz, $^{1}J_{CY}$ = 8.8 Hz), 25.2 (THF-CH$_2$), 21.0 (toluene-*Me*), 12.65 (Cp*-*Me*), 5.48 (NSi*Me*$_3$). ^{31}P{^{1}H} NMR (202 MHz, C_6D_6, 25 °C): δ = 5.9 (d, $^{2}J_{PY}$ = 14.1 Hz). IR ν/cm^{-1}: 2185(w), 1586(w), 1481(w), 1433(m), 1267(m), 1237(m), 1172(w), 1109(m), 1056(m), 1023(m), 996(m), 915(w), 825(s), 802(m), 775(m), 737(s), 709(m), 691(s), 651(m), 631(m), 589(m), 546(m). Elemental analysis calcd (%) for $C_{45}H_{61}N_2OP_2Si_2Y$· 0.5Toluene: C, 64.79; H, 7.29; N, 3.12; found C, 64.21; H, 7.06; N, 3.54.

Synthesis of [Dy{C(PPh$_2$NSiMe$_3$)$_2$}(Cp)(THF)] (**4**).* Step 1: 10 mL of THF was added into a mixture of DyI$_3$(THF)$_{3.5}$ (462 mg, 0.61 mmol) and KBn (158 mg, 1.22 mmol) at 0 °C. After stirring at 0 °C for 4 h, the precipitate was separated by centrifugation and the volatiles were removed under vacuum. The left brown oil was supposed to be "Dy(Bn)$_2$(I)(THF)$_3$" and it was used in the next step without further characterization. Step 2: 5 mL of the toluene solution of CH$_2$(PPh$_2$NSiMe$_3$)$_2$ (323 mg, 0.58 mmol) was added into the 5 mL toluene solution of Dy(Bn)$_2$(I)(THF)$_3$ at −78 °C. After stirring at room temperature for 18 h, the precipitate was separated by centrifugation. The toluene solution was concentrated to a saturated solution and a yellow sediment was deposited. The sediments were isolated and dried under vacuum with a mass of 298 mg, which was supposed to be [Dy{C(PPh$_2$NSiMe$_3$)$_2$}(I)(THF)$_2$] and it was used in the next step without further characterization. Step 3: [Dy{C-(PPh$_2$NSiMe$_3$)$_2$}(I)(THF)$_2$] and KCp* (53 mg, 0.30 mmol) were mixed in a vial with 5 mL of THF. After stirring at room temperature for 2 h and another 8 h at 75 °C, the precipitate was separated by centrifugation. The volatiles were removed under vacuum. The solid was recrystallized from toluene to afford **4** as yellow crystals. Yield: 153 mg, 27%. IR ν/cm^{-1}: 2182(w), 1583(w), 1481(w), 1433(m), 1262(m), 1239(m), 1207(m), 1171(w), 1101(m), 1059(m), 1018(m), 918(w), 822(s), 799(m), 767(m), 734(s), 709(m), 691(s), 651(m), 631(m), 601(m), 548(m). Elemental analysis calcd (%) for $C_{45}H_{61}DyN_2OP_2Si_2$: C, 58.33; H, 6.64; N, 3.02; found C, 59.21; H, 6.53; N2.97.

■ ASSOCIATED CONTENT

Supporting Information

The Supporting Information is available free of charge at https://pubs.acs.org/doi/10.1021/acsomega.4c09784.

NMR spectra of **1**−**3**, crystallographic data of **1**−**4**, magnetic measurement plots of **4**, ab initio calculation of **4** and related references (PDF)

Accession Codes

CCDC 2381767, 2381769, 2381771, and 2381772 contain the supplementary crystallographic data of **1**−**4** for this paper.

■ AUTHOR INFORMATION

Corresponding Author

Chen Wang − *School of Chemistry, Chemical Engineering and Life Science, Wuhan University of Technology, Wuhan 430070 Hubei, P. R. China;* orcid.org/0000-0001-9368-6758; Email: wangchen0@whut.edu.cn

Authors

Fan Li − *School of Chemistry, Chemical Engineering and Life Science, Wuhan University of Technology, Wuhan 430070 Hubei, P. R. China*

Yin-Cong Kong − *School of Chemistry, Chemical Engineering and Life Science, Wuhan University of Technology, Wuhan 430070 Hubei, P. R. China*

Zi Yang − *School of Chemistry, Chemical Engineering and Life Science, Wuhan University of Technology, Wuhan 430070 Hubei, P. R. China*

Complete contact information is available at: https://pubs.acs.org/10.1021/acsomega.4c09784

Notes

The authors declare no competing financial interest.

■ ACKNOWLEDGMENTS

This work was supported by the National Natural Science Foundation of China (Grant No. 22101220) and has been dedicated to Professor Changtao Qian on the occasion of his 90th birthday.

■ REFERENCES

(1) Gao, S. *Molecular Nanomagnets and Related Phenomena*; Springer-Verlag: Berlin, Heidelberg, 2015.

(2) Raju, M. S.; Paillot, K.; Breslavetz, I.; Novitchi, G.; Rikken, G. L. J. A.; Train, C.; Atzori, M. Optical Readout of Single-Molecule Magnets Magnetic Memories with Unpolarized Light. *J. Am. Chem. Soc.* **2024**, *146*, 23616−23624.

(3) Larionova, J.; Guari, Y.; Félix, G. Boosting Single-Molecule Magnet Performance. *Chem* **2024**, *10*, 2351−2353.

(4) Sessoli, R.; Gatteschi, D.; Caneschi, A.; Novak, M. A. Magnetic Bistability in a Metal-Ion Cluster. *Nature* **1993**, *365*, 141−143.

(5) Waldmann, O. A Criterion for the Anisotropy Barrier in Single-Molecule Magnets. *Inorg. Chem.* **2007**, *46*, 10035−10037.

(6) Ruiz, E.; Cirera, J.; Cano, J.; Alvarez, S.; Loose, C.; Kortus, J. Can Large Magnetic Anisotropy and High Spin Really Coexist? *Chem. Commun.* **2008**, 52−54.

(7) Neese, F.; Pantazis, D. A. What Is Not Required to Make a Single Molecule Magnet. *Faraday Discuss.* **2011**, *148*, 229−238.

(8) Aromi, G.; Brechin, E. K. Synthesis of 3d Single Molecule Magnets,. In *Structure and Bonding*; Springer: Berlin, 2006; pp 1−67.

(9) Ishikawa, N.; Sugita, M.; Ishikawa, T.; Koshihara, S.; Kaizu, Y. Lanthanide Double-Decker Complexes Functioning as Magnets at the Single-Molecular Level. *J. Am. Chem. Soc.* **2003**, *125*, 8694−8695.

(10) Benelli, C.; Gatteschi, D. *Introduction to Molecular Magnetism-from Transition Metals to Lanthanides*; Wiley-VCH: Weinheim, 2015.

(11) Woodruff, D. N.; Winpenny, R. E.; Layfield, R. A. Lanthanide Single-Molecule Magnets. *Chem. Rev.* **2013**, *113*, 5110−5148.

(12) Wang, Y.; Luo, Q. C.; Zheng, Y. Z. Organolanthanide Single-Molecule Magnets with Heterocyclic Ligands. *Angew. Chem., Int. Ed.* **2024**, *63*, No. e202407016.

(13) Vieru, V.; Gómez-Coca, S.; Ruiz, E.; Chibotaru, L. F. Increasing the Magnetic Blocking Temperature of Single-Molecule Magnets. *Angew. Chem., Int. Ed.* **2024**, *63*, No. e202303146.

(14) Kragskow, J. G. C.; Mattioni, A.; Staab, J. K.; Reta, D.; Skelton, J. M.; Chilton, N. F. Spin−Phonon Coupling and Magnetic Relaxation in Single-Molecule Magnets. *Chem. Soc. Rev.* **2023**, *52*, 4567−4585.

(15) Ashebr, T. G.; Li, H.; Ying, X.; Li, X.-L.; Zhao, C.; Liu, S.; Tang, J. Emerging Trends on Designing High-Performance Dysprosium(III) Single-Molecule Magnets. *ACS Mater. Lett.* **2022**, *4*, 307−319.

(16) Gould, C. A.; McClain, K. R.; Reta, D.; Kragskow, J. G. C.; Marchiori, D. A.; Lachman, E.; Choi, E.-S.; Analytis, J. G.; Britt, R. D.; Chilton, N. F.; Harvey, B. G.; Long, J. R. Ultrahard magnetism from mixed-valence dilanthanide complexes with metal-metal bonding. *Science* **2022**, *375*, 198−202.

(17) Wang, C.; Meng, Y.-S.; Jiang, S.-D.; Wang, B.-W.; Gao, S. Approaching the uniaxiality of magnetic anisotropy in single-molecule magnets. *Sci. China Chem.* **2023**, *66*, 683−702.

(18) Guo, F. S.; Day, B. M.; Chen, Y. C.; Tong, M. L.; Mansikkamaki, A.; Layfield, R. A. A Dysprosium Metallocene Single-Molecule Magnet Functioning at the Axial Limit. *Angew. Chem., Int. Ed.* **2017**, *56*, 11445−11449.

(19) Goodwin, C. A. P.; Ortu, F.; Reta, D.; Chilton, N. F.; Mills, D. P. Molecular Magnetic Hysteresis at 60 K in Dysprosocenium. *Nature* **2017**, *548*, 439−442.

(20) Burns, C. P.; Wilkins, B. O.; Dickie, C. M.; Latendresse, T. P.; Vernier, L.; Vignesh, K. R.; Bhuvanesh, N. S.; Nippe, M. A Comparative Study of Magnetization Dynamics in Dinuclear Dysprosium Complexes Featuring Bridging Chloride or Trifluoromethanesulfonate Ligands. *Chem. Commun.* **2017**, *53*, 8419−8422.

(21) Randall McClain, K.; Gould, C. A.; Chakarawet, K.; Teat, S. J.; Groshens, T. J.; Long, J. R.; Harvey, B. G. High-Temperature Magnetic Blocking and Magneto-Structural Correlations in a series of Dysprosium(III) Metallocenium Single-Molecule Magnets. *Chem. Sci.* **2018**, *9*, 8492−8503.

(22) Day, B. M.; Guo, F. S.; Layfield, R. A. Cyclopentadienyl Ligands in Lanthanide Single-Molecule Magnets: One Ring To Rule Them All? *Acc. Chem. Res.* **2018**, *51*, 1880−1889.

(23) Guo, F.-S.; Day, B. M.; Chen, Y.-C.; Tong, M.-L.; Mansikkamaki, A.; Layfield, R. A. Magnetic Hysteresis up to 80 K in a Dysprosium Metallocene Single-Molecule Magnet. *Science* **2018**, *362*, 1400−1403.

(24) Liu, J.; Reta, D.; Cleghorn, J. A.; Yeoh, Y. X.; Ortu, F.; Goodwin, C. A. P.; Chilton, N. F.; Mills, D. P. Light Lanthanide Metallocenium Cations Exhibiting Weak Equatorial Anion Interactions. *Chem. - Eur. J.* **2019**, *25*, 7749−7758.

(25) Chen, Y. C.; Liu, J. L.; Ungur, L.; Liu, J.; Li, Q. W.; Wang, L. F.; Ni, Z. P.; Chibotaru, L. F.; Chen, X. M.; Tong, M. L. Symmetry-Supported Magnetic Blocking at 20 K in Pentagonal Bipyramidal Dy(III) Single-Ion Magnets. *J. Am. Chem. Soc.* **2016**, *138*, 2829−2837.

(26) Ding, Y.-S.; Chilton, N. F.; Winpenny, R. E. P.; Zheng, Y.-Z. On Approaching the Limit of Molecular Magnetic Anisotropy: A Near-Perfect Pentagonal Bipyramidal Dysprosium(III) Single-Molecule Magnet. *Angew. Chem., Int. Ed.* **2016**, *55*, 16071−16074.

(27) Wang, C.; Sun, R.; Chen, Y.; Wang, B.-W.; Wang, Z.-M.; Gao, S. Assembling High-Temperature Single-Molecule Magnets with Low-Coordinate Bis(amido) Dysprosium Unit $[DyN_2]^+$ via Cl−K−Cl Linkage. *CCS Chem.* **2020**, *2*, 362−368.

(28) Sun, R.; Li, C.-Y.; Huang, Z.-N.; Wang, C.; Chen, Y.; Sun, H.-L.; Wang, Z.-M.; Wang, B.-W.; Gao, S. One Is Better Than Two: Improved Performance in Mono(imidazolin-2-iminato) Dysprosium(III) Single-Molecule Magnets Featuring Short Dy−N Bond. *CCS Chem.* **2024**, 1.

(29) Xu, W. J.; Luo, Q. C.; Li, Z. H.; Zhai, Y. Q.; Zheng, Y. Z. Bis-Alkoxide Dysprosium(III) Crown Ether Complexes Exhibit Tunable Air Stability and Record Energy Barrier. *Adv. Sci.* **2024**, *11*, No. 2308548.

(30) Lu, E.; Chu, J.; Chen, Y. Scandium Terminal Imido Chemistry. *Acc. Chem. Res.* **2018**, *51*, 557−566.

(31) Wang, C.; Mao, W.; Xiang, L.; Yang, Y.; Fang, J.; Maron, L.; Leng, X.; Chen, Y. Monomeric Rare-Earth Metal Silyl-Thiophosphinoyl-Alkylidene Complexes: Synthesis, Structure, and Reactivity. *Chem. - Eur. J.* **2018**, *24*, 13903−13917.

(32) Liddle, S. T.; Mills, D. P.; Wooles, A. J. Early Metal Bis(phosphorus-stabilised)carbene Chemistry. *Chem. Soc. Rev.* **2011**, *40*, 2164−2176.

(33) Gregson, M.; Lu, E.; Mills, D. P.; Tuna, F.; McInnes, E. J. L.; Hennig, C.; Scheinost, A. C.; McMaster, J.; Lewis, W.; Blake, A. J.; Kerridge, A.; Liddle, S. T. The Inverse-Trans-Influence in Tetravalent Lanthanide and Actinide Bis(carbene) Complexes. *Nat. Commun.* **2017**, *8*, No. 14137.

(34) Gregson, M.; Chilton, N. F.; Ariciu, A.-M.; Tuna, F.; Crowe, I. F.; Lewis, W.; Blake, A. J.; Collison, D.; McInnes, E. J. L.; Winpenny, R. E. P.; Liddle, S. T. A Monometallic Lanthanide Bis(methanediide) Single Molecule Magnet with a Large Energy Barrier and Complex Spin Relaxation Behaviour. *Chem. Sci.* **2016**, *7*, 155−165.

(35) Thomas-Hargreaves, L. R.; Giansiracusa, M. J.; Gregson, M.; Zanda, E.; O'Donnell, F.; Wooles, A. J.; Chilton, N. F.; Liddle, S. T. Correlating Axial and Equatorial Ligand Field Effects to the Single-Molecule Magnet Performances of a Family of Dysprosium Bis-Methanediide Complexes. *Chem. Sci.* **2021**, *12*, 3911−3920.

(36) Mills, D. P.; Wooles, A. J.; McMaster, J.; Lewis, W.; Blake, A. J.; Liddle, S. T. Heteroleptic $[M(CH_2C_6H_5)_2(I)(THF)_3]$ Complexes (M = Y or Er): Remarkably Stable Precursors to Yttrium and Erbium T-Shaped Carbenes. *Organometallics* **2009**, *28*, 6771−6776.

(37) Liddle, S. T.; McMaster, J.; Green, J. C.; Arnold, P. L. Synthesis and Structural Characterisation of an Yttrium-Alkyl-Alkylidene. *Chem. Commun.* **2008**, 1747−1749.

(38) Mills, D. P.; Cooper, O. J.; McMaster, J.; Lewis, W.; Liddle, S. T. Synthesis and Reactivity of the Yttrium-Alkyl-Carbene Complex $[Y(BIPM)(CH_2C_6H_5)(THF)]$ (BIPM = $\{C(PPh_2NSiMe_3)_2\}$). *Dalton Trans.* **2009**, 4547−4555.

(39) Mills, D. P.; Soutar, L.; Cooper, O. J.; Lewis, W.; Blake, A. J.; Liddle, S. T. Reactivity of the Yttrium Alkyl Carbene Complex $[Y(BIPM)(CH_2C_6H_5)(THF)]$ (BIPM = $\{C(PPh_2NSiMe_3)_2\}^{2-}$): From Insertions, Substitutions, and Additions to Nontypical Transformations. *Organometallics* **2013**, *32*, 1251−1264.

https://doi.org/10.1021/acsomega.4c09784
ACS Omega 2024, 9, 50830−50837

(40) Ortu, F.; Gregson, M.; Wooles, A. J.; Mills, D. P.; Liddle, S. T. Yttrium Methanide and Methanediide Bis(silyl)amide Complexes. *Organometallics* **2017**, *36*, 4584−4590.

(41) Wooles, A. J.; Cooper, O. J.; McMaster, J.; Lewis, W.; Blake, A. J.; Liddle, S. T. Synthesis and Characterization of Dysprosium and Lanthanum Bis(iminophosphorano)methanide and -methanediide Complexes. *Organometallics* **2010**, *29*, 2315−2321.

(42) Evans, W. J.; Meadows, J. H.; Wayda, A. L.; Hunter, W. E.; Atwood, J. L. Organolanthanide Hydride Chemistry. 1. Synthesis and X-ray Crystallographic Characterization of Dimeric Organolanthanide and Organoyttrium Hydride Complexes. *J. Am. Chem. Soc.* **1982**, *104*, 2008−2014.

(43) Thim, R.; Dietrich, H. M.; Bonath, M.; Maichle-Mössmer, C.; Anwander, R. Pentamethylcyclopentadienyl-Supported Rare-Earth-Metal Benzyl, Amide, and Imide Complexes. *Organometallics* **2018**, *37*, 2769−2777.

(44) Long, J.; Tolpygin, A. O.; Cherkasov, A. V.; Lyssenko, K. A.; Guari, Y.; Larionova, J.; Trifonov, A. A. Single-Molecule Magnet Behavior in Dy^{3+} Half-Sandwich Complexes Based on Ene-Diamido and Cp* Ligands. *Organometallics* **2019**, *38*, 748−752.

(45) Lin, S. Y.; Zhao, L.; Guo, Y. N.; Zhang, P.; Guo, Y.; Tang, J. Two New Dy3 Triangles with Trinuclear Circular Helicates and Their Single-Molecule Magnet Behavior. *Inorg. Chem.* **2012**, *51*, 10522−10528.

(46) Izod, K.; Liddle, S. T.; Clegg, W. A Convenient Route to Lanthanide Triiodide THF Solvates. Crystal Structures of $LnI_3(THF)_4$ [Ln = Pr] and $LnI_3(THF)_{3.5}$ [Ln = Nd, Gd, Y]. *Inorg. Chem.* **2004**, *43*, 214−218.

(47) Schlosser, M.; Hartmann, J. Transmetalation and Double Metal Exchange: A Convenient Route to Organolithium Compounds of the Benzyl and Allyl Type. *Angew. Chem., Int. Ed.* **1973**, *12*, 508−509.

(48) Callebaut, B.; Hullaert, J.; Van Hecke, K.; Winne, J. M. An Intramolecular Cycloaddition Approach to the Kauranoid Family of Diterpene Metabolites. *Org. Lett.* **2019**, *21*, 310−314.

(49) Evans, W. J.; Kozimor, S. A.; Ziller, J. W.; Kaltsoyannis, N. Structure, Reactivity, and Density Functional Theory Analysis of the Six-Electron Reductant, $[(C_5Me_5)_2U]_2(\mu\text{-}\eta^6\text{:}\eta^6\text{-}C_6H_6)$, Synthesized via a New Mode of $(C_5Me_5)_3M$ Reactivity. *J. Am. Chem. Soc.* **2004**, *126*, 14533−14547.

(50) Appel, R.; Ruppert, I. Darstellung silylierter Alkylen-bisiminophosphorane und ihre Cyclisierung mit Phosphor(V)-fluoriden. *Z. Anorg. Allg. Chem.* **1974**, *406*, 131−144.

(51) Petrov, A. R.; Derheim, A.; Oetzel, J.; Leibold, M.; Bruhn, C.; Scheerer, S.; Oßwald, S.; Winter, R. F.; Siemeling, U. A Stable Planar-Chiral N-Heterocyclic Carbene with a 1,1′-Ferrocenediyl Backbone. *Inorg. Chem.* **2015**, *54*, 6657−6670.

https://doi.org/10.1021/acsomega.4c09784
ACS Omega 2024, 9, 50830−50837